10th ANKARA INTERNATIONAL AEROSPACE CONFERENCE AIAC-2019-171
18-20 September 2019 - METU, Ankara TURKEY

LARGE EDDY SIMULATION OF A DUCTED WIND TURBINE FOR AEROACOUSTIC PREDICTIONS

Emre Alpman[1]
Marmara University
Istanbul, Turkey

Levent A. Kavurmacıoğlu[2]
Istanbul Technical University
Istanbul, Turkey

ABSTRACT

This paper includes a large eddy simulation around a ducted wind turbine for aeroacoustics predictions. The geometry of the turbine was previously aerodynamically optimized for maximum annual energy production at minimum drag force. Dynamic meshes are used to handle the rotating and stationary flow domains containing the rotor and the duct, and the numerical solutions are obtained using the ***pimpleDyMFoam*** *solver of the open source computational fluid dynamics software* ***OpenFOAM****. Acoustics predictions will be performed for 13 probe points located around the turbine using the* ***noise*** *post processing utility of OpenFOAM. Predictions obtained for the ducted rotor will be presented and compared with those obtained for the rotor without the duct.*

INTRODUCTION

Small or micro-scale wind turbines are typically employed in urban areas mainly due to lack of available space for large wind turbines [Kaldellis et al. 2012; Cace et al. 2007; Grant et al. 2008; Mertens, 2006]. Since power produced by a wind turbine is proportional to its rotor area, the power production of the turbine decreases considerably when its size becomes smaller [Burton et.al, 2011]. This problem can be alleviated by increasing the wind speed experienced by the rotor because the power production is also proportional to the cube of the wind speed [Burton et.al, 2011]. Placing a rotor inside a duct increases the mass flow rate through the rotor; hence it improves the performance of the turbine [Gomis, 2011; Hansen et al. 2000; Alpman, 2018.a]. However, the presence of the duct also increases the drag force acting on the turbine [Gomis, 2011; Hansen et al. 2000; Wang and Shen, 2008; Alpman, 2018.a]. Although a with a multiobjective optimization methodology it becomes possible to produce power at a minimum possible drag force, it would still be higher compared to a bare rotor at the same rotor radius [Alpman, 2018.a]. In addition to this, since a wind turbine in an urban environment would operate close to people, it is also desired to be quiet [Wagner et al. 2012; Pedersen and Waye, 2004; Pedersen and Waye, 2007]. The aim of this study is therefore to predict the aerodynamic noise emitted by a ducted wind turbine, which was

[1] Assoc. Prof. Dr. in Mechanical Engineering Department, Email: emre.alpman@marmara.edu.tr
[2] Assoc. Prof. Dr. in Mechanical Engineering Department, Email: kavurmacio@itu.edu.tr

previously optimized aerodynamically for maximum annual energy production at the minimum possible drag force [Alpman, 2018.a]. In the field of computational aeroacoustics (CAA) aerodynamic noise can either be predicted directly by resolving the full spectrum of fluctuations everywhere in the flow domain using direct numerical simulation (DNS) or using a so called hybrid methodology which involves the solution of Navier-Stokes equation in the near field and a linear acoustic solver for the far-field region where the non-linearities are assumed to disappear [Wagner et. al, 2007]. Since the former approach is computationally intensive, the latter approach is typically used for CAA predictions [Wagner et. al, 2007, Kurultay and Alpman, 2016]. Propagation of noise involves wave motion; therefore the flow field should be modeled using a compressible flow solver [Wagner et. al, 2007]. Compressible large eddy simulation (LES), which can simulate complex turbulent flows involving wave motion, can be successfully used for aeroacoustics predictions [Wagner et. al, 2007; Alpman, 2018.b, Alpman and Soylemez, 2018]. However, the presence of the speed of sound in the definition of Courant number for compressible flows [Anderson et al. 2016] was shown to place severe restrictions on the time step used in the simulations when the flow Mach number is low [Alpman and Soylemez, 2018]. Hence, an incompressible LES approach is selected for flow simulations in this study. Even though the incompressible pressure fluctuations are different than acoustic pressure fluctuations [Kaltenbacher, 2018], they can be used as the source term for the acoustic analogies based on the Lighthill's inhomogeneous wave equation [Kaltenbacher, 2018]. This approach has been successfully applied for aeroacoustics predictions for wind turbines [Ghasemian and Nejat, 2015; Wasala et al. 2015].

The geometry of the ducted wind turbine analyzed in this study is shown in Figure 1. The rotor, with a diameter of 1m, is composed of four blades, each having the S833 airfoil section (https://wind.nrel.gov/airfoils/shapes/S833_Shape.html). The duct has an airfoil shaped cross-section whose shape was previously optimized along with the blade geometry, number of blades and the position of the rotor relative to the duct for annual energy production [Alpman, 2018.a]. The turbine is placed in a uniform wind of 6 m/s and the blades are made to rotate at a constant angular speed of 200 rpm. In addition to the simulations performed for the ducted turbine shown in Figure 1, aeroacoustics predictions are also performed and presented for the rotor-only configuration.

METHODOLOGY

The turbulent flow field around the turbine is simulated using (LES) the numerical solutions are performed using the open source computational fluid dynamics software OpenFOAM. Here, the sub-grid scale (SGS) stresses are computed via the *kEqn* model of the software which models the SGS stresses using a one-equation eddy viscosity model [Alpman, 2018.b]. Computational mesh required for the solutions is constructed using the open source meshing software *cfMesh*. Since the flow domain will include rotating blades and a stationary duct; multiple sub-domains, one rotating and one stationary, is constructed. These domains are meshed separately and then they are combined using the *mergeMeshes* utility of OpenFOAM. This utility generates an interface between the domains on which an arbitrary mesh interface (AMI) boundary condition is applied. In [Alpman, 2018.a] where CFD solutions had also been performed for ducted rotors, frozen rotor approach was followed by defining multiple rotating reference frames for the rotating and stationary domains. For the rotor-only solutions same rotating and stationary sub-domains are used, however, the stationary domain does not contain the duct geometry for this case. Inside the rotating domain which contains the rotor, the maximum cell length is limited by 5mm where this limit is reduced to 1mm in the vicinity of the blades. This way the computational meshes for both the ducted and the rotor-only cases consist of more than 6.5 million cells.

The *pimpleDyMFoam* solver of OpenFOAM is used for the numerical solutions because it can handle dynamic meshes for incompressible flows. The overall flow domain has the shape of a cylinder whose longitudinal axis coincides with the flow direction. At the inlet of the domain flow speed is set to 6 m/s while the pressure is set to its atmospheric value at the outlet. Freestream conditions are applied at the lateral surface of the domain. No-slip boundary conditions are applied on the solid surfaces along with a wall function for the SGS turbulent kinetic energy because the mesh normal to the solid surfaces is not fine enough to resolve the turbulent boundary layer. At the sliding interface between the rotating and stationary domains *cyclicAMI* boundary condition of OpenFOAM is used for flow data transfer.

In this study the acoustic predictions are performed using the *noise* post processing utility of OpenFOAM. Here, the instantaneous pressure is recorded at 13 probe points located around the turbine. The locations of these probe points relative to the ducted turbine are shown in Figure 2. The probe points are located on the *xy*-plane (see the coordinate axes in Figure 1) and on the upper half of the flow domain.

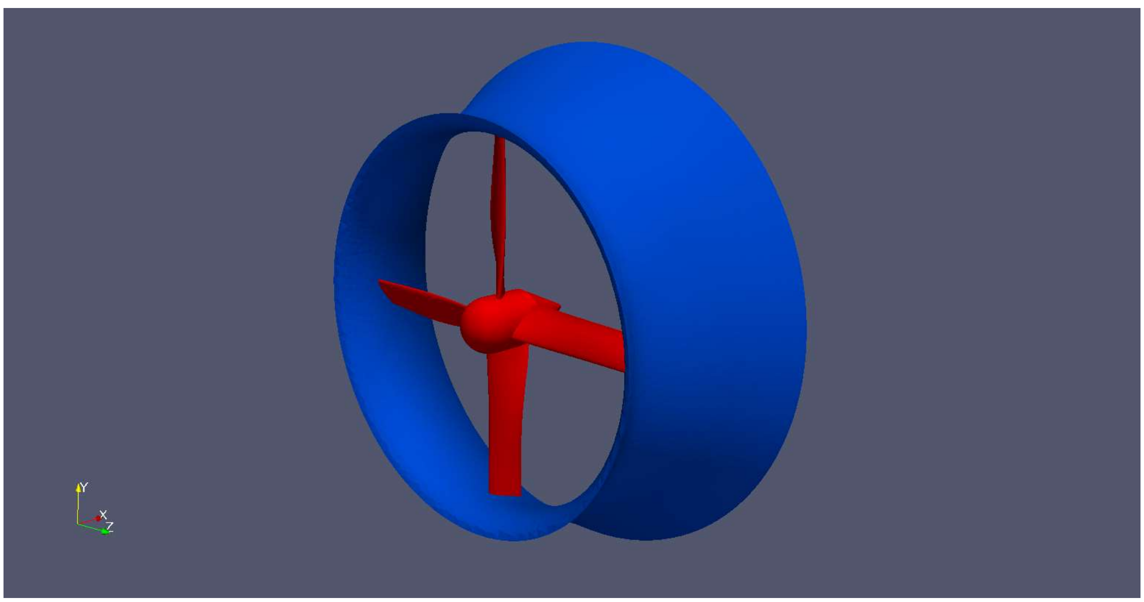

Figure 1 Duct and the rotor geometry

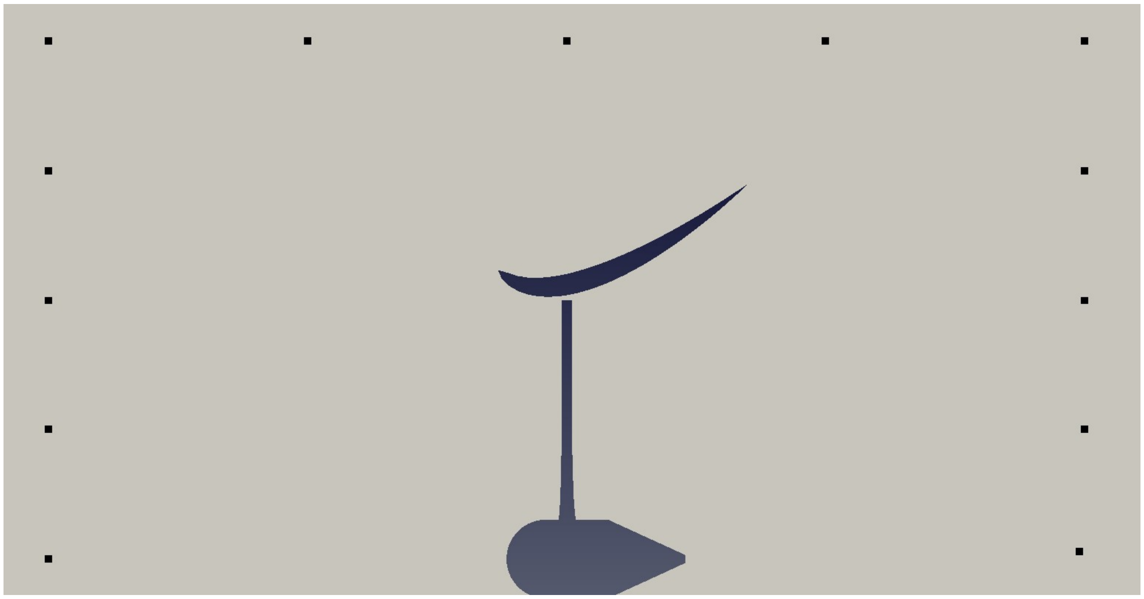

Figure 2 Probe points (shown as black squares) relative to the ducted turbine

RESULTS AND DISCUSSION

Results are obtained for a ducted wind turbine, whose geometry was previously optimized aerodynamically [Alpman, 2018.a]. Here, the freestream wind speed is 6 m/s and the rotor rotates at a constant angular speed of 200 rpm. The flow domain surrounding the rotor rotates with it, while the outer flow domain which includes the duct and the farfield regions is stationary. At the sliding interface between them *cyclicAMI* boundary condition of OpenFOAM is used for flow data transfer.

Numerical solutions for the ducted turbine and rotor-only cases are performed for 0.1024 seconds of real time. At the angular speed of 200 rpm this corresponds to a 122.88° of rotation of the blades from their original position. Unfortunately, this is not even close to a single revolution of the rotor. However, the time step used in the simulations was on the order of 1μs and applying the *cyclicAMI* condition across the sliding interface slowed down the computations. Therefore, the numerical simulations required considerable amount of computational time. During the computations, flow field was stored at every 2ms so that at the end 512 pressure recordings could be collected for the Fast Fourier Transform (FFT) performed by the *noise* utility.

Figure 3 displays the iso-vorticity surface around the duct and the rotor obtained at t = 0.07 s. For clarity the rotor and the duct are colored with red and only the half of the duct and the iso-vorticity surface are displayed. At this time the rotors rotated about 84 degrees from its original position and the iso-vorticity around the duct, rotor blades and in the rotor wake are evident.

Contours of fluid speed on the z = 0 plane at t = 0.0256, 0.0512, 0.0768 and 0.1024 s obtained for the rotor-only (left) and ducted (right) cases are displayed in Figure 4. The effect of the blade movement on the flow field can be clearly seen from this figure. Also the flow variables seem to be smoothly transferred between the rotating and stationary flow domains. Compared to the rotor-only case, the presence of the duct clearly increases the wind speed upstream of the rotor and it also decreases the fluid speed, and the fluid momentum, downstream of the rotor. This is an expected result because the presence of the duct improves the power production [Alpman, 2018.a].

Pressure fluctuations about the mean value obtained at on the z = 0 plane at t = 0.0256, 0.0512, 0.0768 and 0.1024 s are displayed in Figure 5. Here, the pressure fluctuations are obtained by subtracting the mean value of the pressure from its instantaneous value. The mean value of pressure at any time is calculated by time averaging pressure from the initial time to that particular time. When the images of Figure 5 are investigated it can be seen that the duct creates strong positive fluctuations at initial times, which weaken as time goes on. The oval-like negative fluctuation regions shown in this figure denote the presence of vortex structures. It is clear that the duct suppresses the tip vortices while its presence strengthens the hub vortices. Looking at these pressure fluctuation snapshots one can conclude that while the presence of the duct improves the power production performance of the turbine, it would make it noisier compared to the rotor-only case.

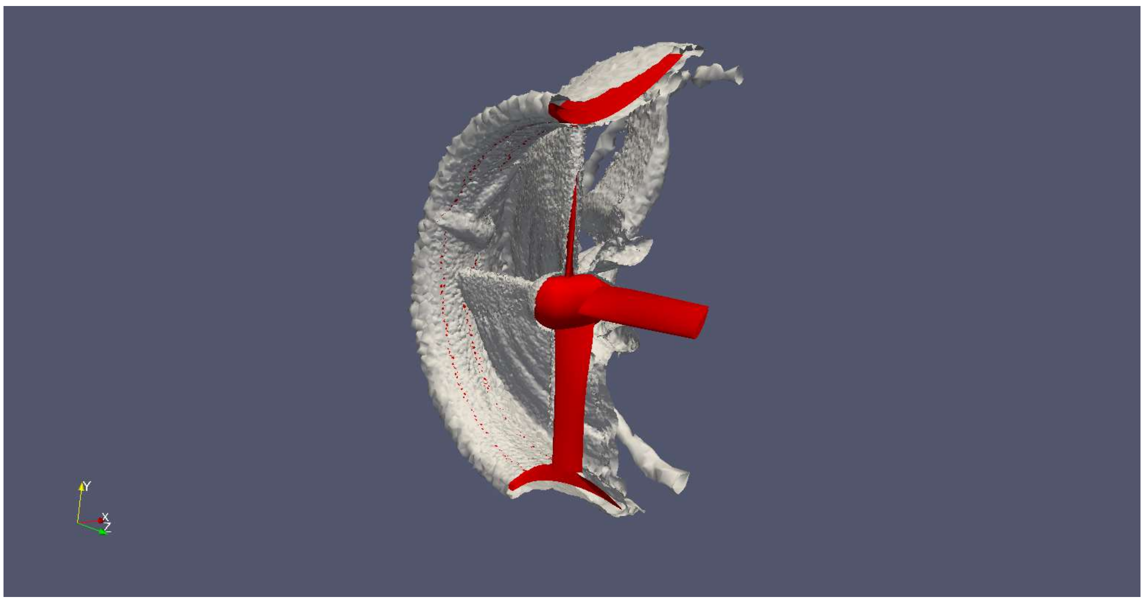

Figure 3 Iso-vorticity contours around the duct and the rotor (t = 0.07 s)

In order to compare the acoustic performance of the ducted turbine with that of the rotor-only turbine the pressure data collected at the probe points shown in Figure 2 are submitted in to the *noise* utility of OpenFOAM. The probe points are numbered starting from 1 for the point at the lower left corner of Figure 2 and increase in a counter-clockwise manner. The sound pressure spectra obtained using the *noise* utility at different probe locations are shown in Figure 6. Note that, the probes 1, 3, 5 are upstream, 9, 11, 13 are downstream of the turbine while the probe 7 lies on the top. At all probe locations the spectra have broadband nature and there are no visible harmonics. However, this may be due to the shortness of the simulation time. These results need or the utility employed are not validated using measurements. Still the authors believe that they can be used for comparison purposes. Nevertheless at all locations the ducted turbine is shown to be noisier than the rotor-only case. The difference seems to decrease at downstream probe locations.

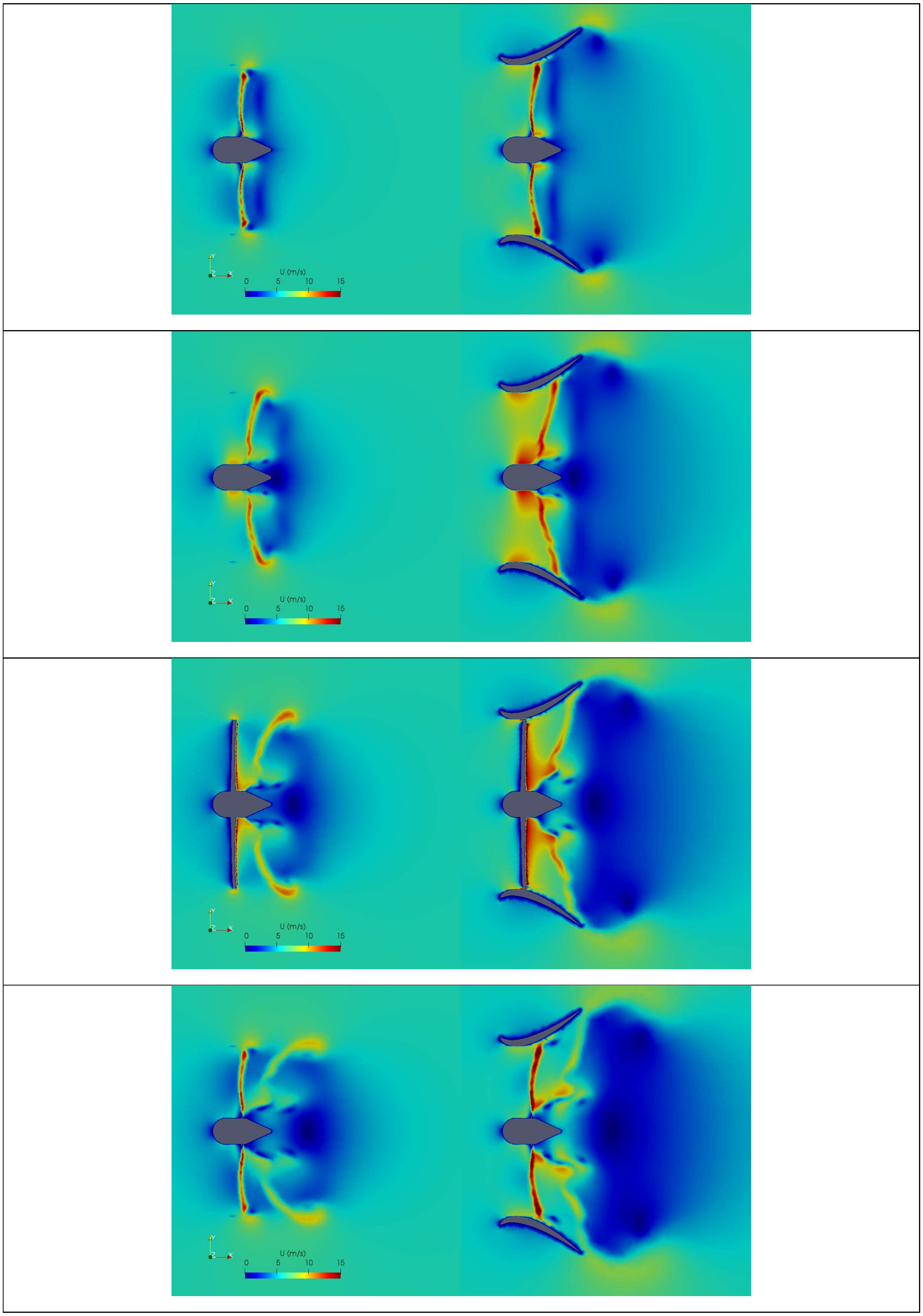

Figure 4 Velocity contours at z = 0 plane at different times.

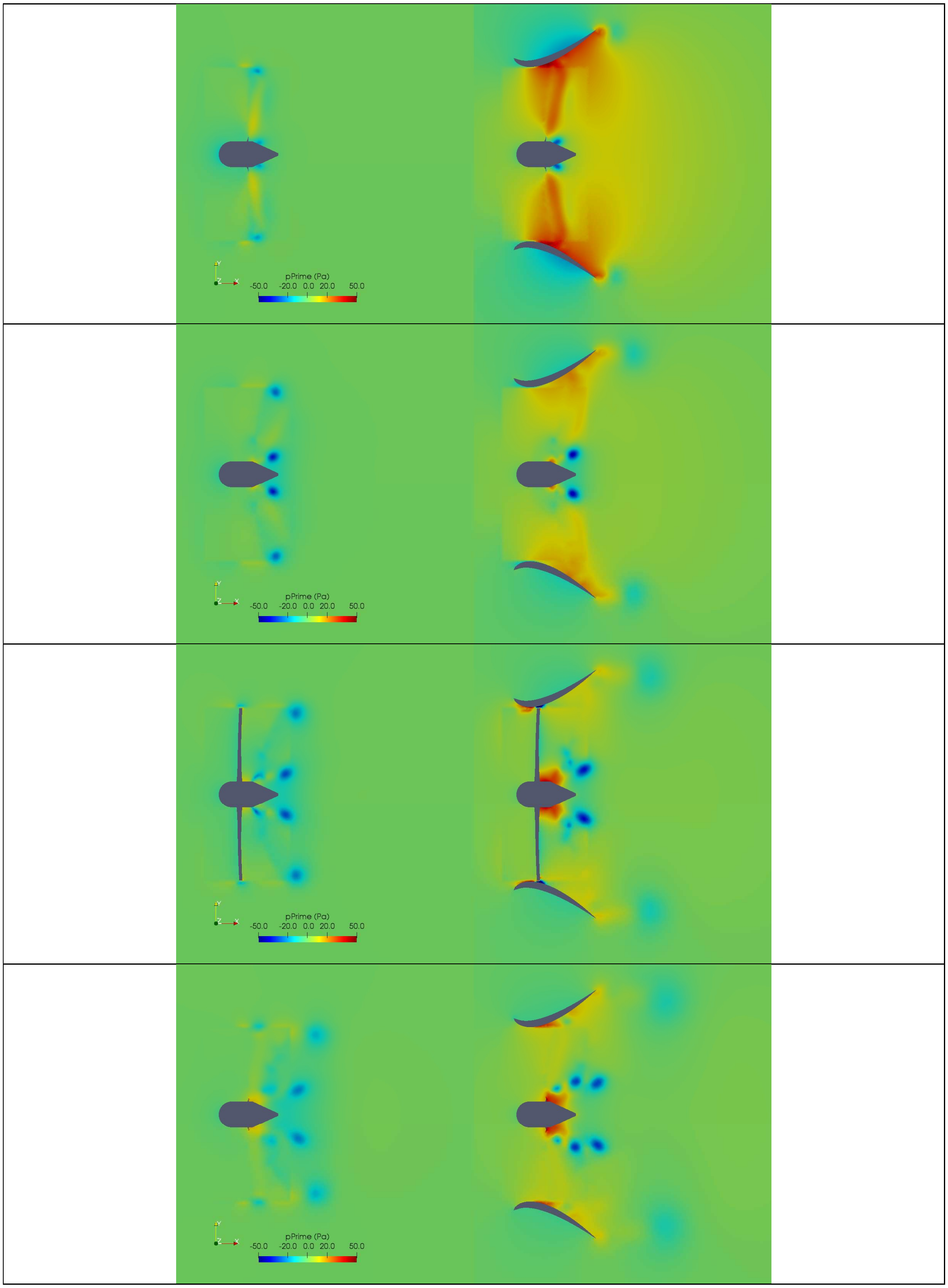

Figure 5 Pressure fluctuations about the mean pressure at different times

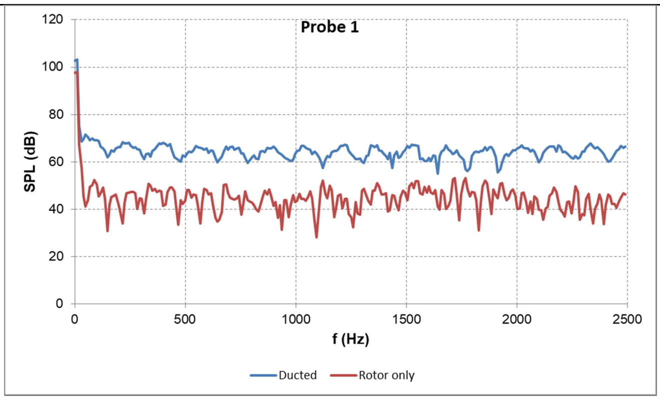
Probe 1
SPL (dB)
f (Hz)
Ducted
Rotor only

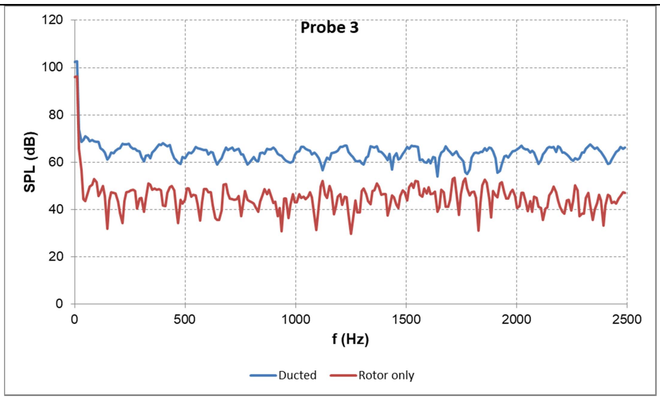
Probe 3
SPL (dB)
f (Hz)
Ducted
Rotor only

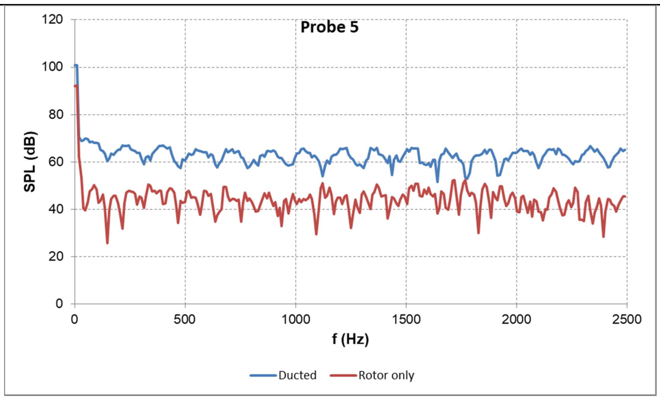
Probe 5
SPL (dB)
f (Hz)
Ducted
Rotor only

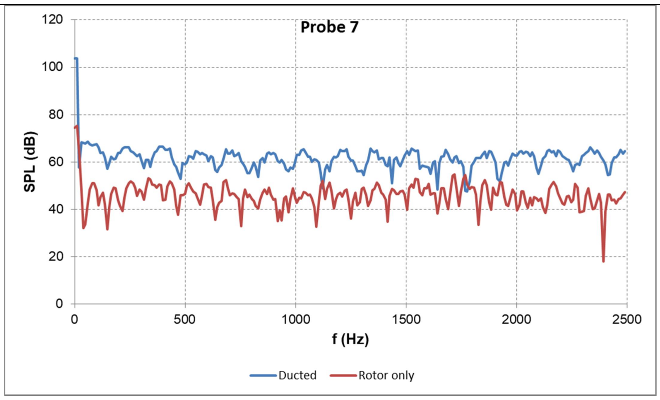
Probe 7
SPL (dB)
f (Hz)
Ducted
Rotor only

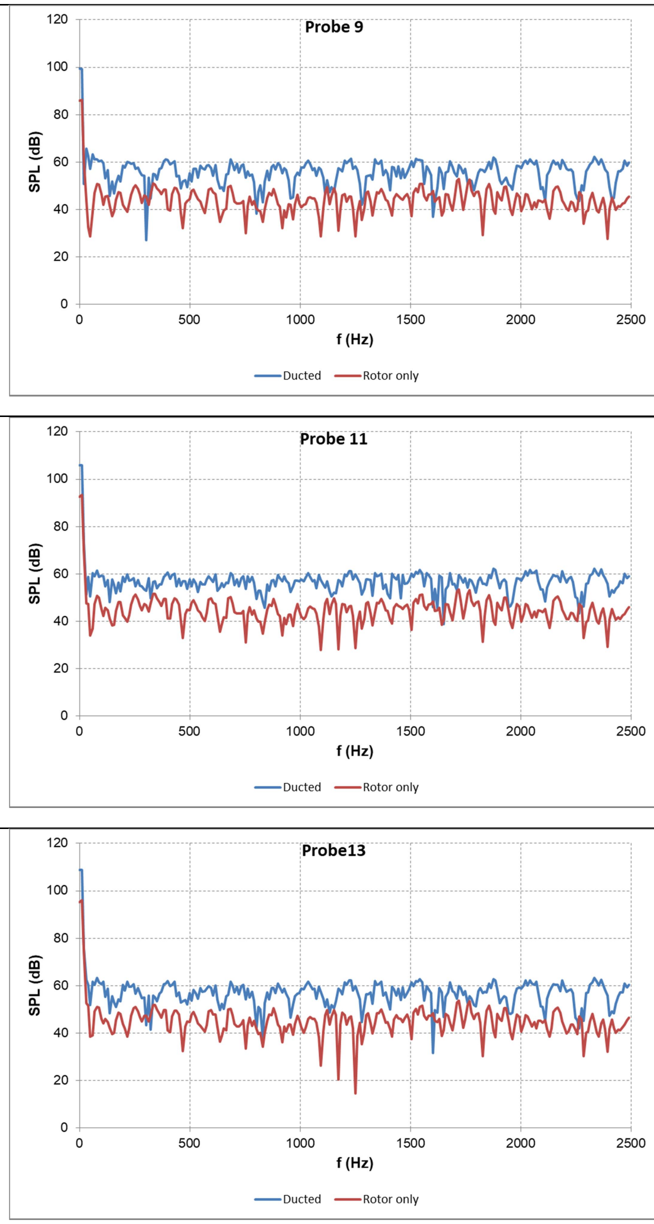

Figure 6 Sound pressure level (SPL) spectra at different probe locations.

The predictions displayed in Figure 6 show that placing a duct around a turbine would successfully increase the power production however, at the expense of increased drag force [Alpman, 2018.a] and noise. Therefore, during the aerodynamic optimization process of a ducted wind turbine a three-objective optimization process with annual energy production, drag force and aerodynamic noise as objective functions. Here, the optimizer would maximize the first while minimizing the second and the third objectives.

CONCLUSIONS

LES predictions around a ducted wind turbine and rotor-only wind turbine were performed I order to make aeroacoustics predictions. The geometry of the turbine was previously aerodynamically optimized for maximum annual energy production at minimum drag force [Alpman, 2018.a]. The solution domain consisted of a rotating domain containing the rotor and a stationary domain surrounding it with a sliding mesh interface in between. The numerical solutions were performed using the *pimpleDyMFoam* solver of OpenFOAM which can handle dynamic meshed for incompressible flows. The cyclicAMI boundary condition of the software was applied at the sliding interface. The following conclusions could be drawn from the results presented in this paper:

- Even though it improves power production, the presence of the duct increases the pressure fluctuations, hence the aerodynamic noise, around the turbine in addition to the total drag force applied.
- The difference between the SPL spectra of ducted and rotor-only turbines turned out to be lower at downstream of the turbine compared to the upstream and side locations.
- The noise production can be included to aerodynamic optimization process of a ducted wind turbine as an objective to be minimized when such wind turbines are planned to be located in urban areas.

The authors also planned to perform aeroacoustics simulations using the libAcoustics (https://github.com/unicfdlab/libAcoustics), which is a library developed for OpenFOAM for far field noise prediction. However, the library was compatible with OpenFOAM version 4.0, which is a slightly older version of the software and unfortunately it was not compatible with Ubuntu 18.04 LTS, the operating system on the computer where the numerical solutions were performed. Therefore, extending the compatibility of this library to the newer OpenFOAM versions is recommended as a future work.

References

Alpman, E. (2018.a). *Multiobjective aerodynamic optimization of a microscale ducted wind turbine using a genetic algorithm*. Turkish Journal of Electrical Engineering & Computer Sciences, 26(1), 618-629.

Alpman, E. (2018.b) *Large Eddy Simulation and Aeroacoustic Analysis for Simple Expansion Silencer Like Geometries*. International Journal of Advances on Automotive and Technology, 2 (3), 168 – 174.

Alpman, E., Söylemez, E. (2018) *Aeroacoustic Analysis of an Air-Reed Instrument Using Large Eddy Simulation* 4th International Conference on Advances In Mechanical Engineering (ICAME 2018).

Anderson, D., Tannehill, J. C., & Pletcher, R. H. (2016). Computational fluid mechanics and heat transfer. CRC Press.

Burton, T., Jenkins, N., Sharpe, D., & Bossanyi, E. (2011). *Wind energy handbook*. John Wiley & Sons.

Cace J, ter Horst RE, Syngellakis HK, Power IT. (2007) Urban Wind Turbines. Guidelines for Small Wind Turbines in the Built Environment. Brussels, Belgium: Wineur Intelligent Energy Europe.

Ghasemian, M., & Nejat, A. (2015). *Aero-acoustics prediction of a vertical axis wind turbine using Large Eddy Simulation and acoustic analogy*. Energy, 88, 711-717.

Gomis L. L. (2011) Effect of diffuser augmented micro wind turbines features on device performance. MSc, University of Wollongong, Wollongong, Australia.

Grant A, Johnstone C, Kelly N. (2008) Urban wind energy conversion: the potential of ducted turbines. Renew Energ. 33, 1157-1163.

Hansen M.O.L, Sorensen N.N, Flay R.G.J. (2000) Effect of placing a diffuser around a wind turbine. Wind Energy.; 3, 207-213.

Kaldellis J, Zarakis D, Kondili E, Papapostolou C. (2012) *Trends, prospects and R&D directions of the global wind energy sector*. EWEA 2012 Annual Event. pp. 1403-1411.

Kaltenbacher, M. (Ed.). (2018). *Computational Acoustics*. Springer International Publishing.

Kurultay, A. A., Alpman, E., (2016) *Prediction of Horizontal Axis Wind Turbine Acoustics* Marmara University Journal of Institute of Pure and Applied Sciences, 28 (1), 35 – 48.

Mertens S. (2006) *Wind energy in the built environment: concentrator effects of buildings*. PhD, Delft University of Technology, Delft, the Netherlands.

Pedersen, E., & Waye, K. P. (2004). *Perception and annoyance due to wind turbine noise—a dose–response relationship.* The Journal of the Acoustical Society of America, 116(6), 3460-3470.

Pedersen, E., & Waye, K. P. (2007). *Wind turbine noise, annoyance and self-reported health and well-being in different living environments*. Occupational and environmental medicine, 64(7), 480-486.

Wagner, C., Hüttl, T., & Sagaut, P. (Eds.). (2007). *Large-eddy simulation for acoustics* (Vol. 20). Cambridge University Press.

Wagner, S., Bareiss, R., & Guidati, G. (2012). *Wind turbine noise*. Springer Science & Business Media.

Wang SH, Chen SH. (2008) *Blade number effect for a ducted wind turbine*. J Mech Sci Technol., 22, 1984-1992.

Wasala, S. H., Storey, R. C., Norris, S. E., & Cater, J. E. (2015). *Aeroacoustic noise prediction for wind turbines using Large Eddy Simulation*. Journal of Wind Engineering and Industrial Aerodynamics, 145, 17-29.